



Synthesis of Doxorubicin loaded magnetic chitosan nanoparticles for pH responsive targeted drug delivery



Gozde Unsoy^{a,*}, Rouhollah Khodadust^{a,1}, Serap Yalcin^{b,1}, Pelin Mutlu^c, Ufuk Gunduz^{a,*}

^a Middle East Technical University, Department of Biotechnology, 06800 Ankara, Turkey

^b Ahi Evran University, Department of Food Engineering, 40000 Kırşehir, Turkey

^c Middle East Technical University, Central Laboratory, Molecular Biology and Biotechnology R&D Center, 06800 Ankara, Turkey

ARTICLE INFO

Article history:

Received 11 February 2014

Received in revised form 30 April 2014

Accepted 26 May 2014

Available online 12 June 2014

Keywords:

Targeted drug delivery

Doxorubicin

Chitosan

Magnetic nanoparticles

ABSTRACT

Targeted drug delivery is a promising alternative to overcome the limitations of classical chemotherapy. In an ideal targeted drug delivery system carrier nanoparticles would be directed to the tumor tissue and selectively release therapeutic molecules. As a novel approach, chitosan coated magnetic nanoparticles (CS MNPs) maintain a pH dependent drug delivery which provides targeting of drugs to the tumor site under a magnetic field. Among various materials, chitosan has a great importance as a pH sensitive, natural, biodegradable, biocompatible and bioadhesive polymer. The aim of this study was to obtain an effective targeted delivery system for Doxorubicin, using chitosan coated MNPs. Different sized CS MNPs were produced by in situ synthesis method. The anti-cancer agent Doxorubicin was loaded onto CS MNPs which were characterized previously. Doxorubicin loading was confirmed by FTIR. Drug loading and release characteristics, and stability of the nanoparticles were investigated. Our results showed that the CS MNPs have pH responsive release characteristics. The cellular internalization of Doxorubicin loaded CS MNPs were visualized by fluorescent microscopy. Doxorubicin loaded CS MNPs are efficiently taken up by MCF-7 (MCF-7/S) and Doxorubicin resistant MCF-7 (MCF-7/1 μM) breast cancer cells, which increases the efficacy of drug and also maintains overcoming the resistance of Doxorubicin in MCF-7/Dox cells. Consequently, CS MNPs synthesized at various sizes can be effectively used for the pH dependent release of Doxorubicin in cancer cells. Results of this study can provide new insights in the development of pH responsive targeted drug delivery systems to overcome the side effects of conventional chemotherapy.

© 2014 Elsevier B.V. All rights reserved.

1. Introduction

Magnetic nanoparticles (MNPs), which can be targeted to tumor site in a magnetic field, gained importance in cancer therapy in recent years. Targeted delivery of drug by nanoparticles can overcome difficulties associated with conventional chemotherapeutic agents, including insolubility under aqueous conditions, rapid clearance, and a lack of selectivity, resulting in nonspecific toxicity toward normal cells (Maeda, 2001). Moreover, drug resistance can be overcome when chemotherapeutic drugs are given as loaded on nanoparticles to breast cancer cells while free drug is pumped out by resistance mechanisms of the cell (Zeng et al., 2014).

Drug loaded nanoparticles are able to penetrate tumors due to their small size, and the leaky nature of tumor microvasculature (Strebhardt and Ullrich, 2008). Furthermore, poor lymphatic

drainage of tumor microenvironment results in slow clearance of nanoparticles and their accumulation in tumor microenvironment (Liu et al., 2008).

MNPs include metallic, bimetallic, and superparamagnetic iron oxide nanoparticles, which have reactive surface that can be coated with biocompatible polymers and loaded with therapeutic agents (Sun et al., 2008). There are several commercially available MNP-based drugs, which were approved for various biomedical applications (Gupta et al., 2007).

Chitosan has important structural and biological properties, which include the cationic character and the solubility in aqueous medium. Its biodegradability and mucoadhesivity are the other advantages (Dash et al., 2011). Chitosan is soluble at acidic solutions owing to the protonation of the amino groups in the polymeric chain (Rodrigues et al., 2012).

The chitosan coating is preferable to modify the surface properties of the core structure, either to improve the pattern of interaction with surrounding structures or to improve the biodegradation profile (Andrade et al., 2011; Grenha, 2012). Chitosan has an intrinsic anti-tumor activity, stimulating the production of

* Corresponding authors. Tel.: +90 536 612 69 39; fax: +90 312 210 79 76.

E-mail addresses: gozdeunsoy@hotmail.com (G. Unsoy), ufukg@metu.edu.tr (U. Gunduz).

¹ Co-authors equally contributed for this manuscript.

Tissue Necrotic Factor- α (TNF- α) by monocytes. Besides, chitosan molecules demonstrated a good retention in the blood circulation and a slight accumulation in tissues, suggesting that it can be an effective carrier for drugs that are excreted rapidly (Dodane and Vilivalam, 1998).

In tumor cells, low pH values, such as pH 5.5 are generated by the anaerobic glucose metabolism. After targeting of nanoparticles to the tumor site drug release starts at the acidic microenvironment of the tumor tissue. pH responsive chitosan nanoparticles would be expected to have an effective drug release in the tumor microenvironment since the drug release rate can be suddenly accelerated with lower pH (Aydin and Pulat, 2012). Moreover, pH values of 3.0–5.5 are seen in acidic intracellular organelles, such as endosomes and lysosomes, within the cells (Lim et al., 2011). Further release of drug continues in these acidic organelles inside the cells.

The water-soluble anti-cancer drug Doxorubicin is one of the most commonly used anti-cancer drug for the treatment of many cancer types (Wood, 2002). Doxorubicin is a strong cytotoxic compound to normal tissues and its cardiac toxicity has also been well documented by several groups (Longhi et al., 2007). To decrease the toxicity of Doxorubicin, targeted delivery of the drug through polymeric nanoparticles is an alternative option for cancer therapy (Tan et al., 2009).

In this study, chitosan coated magnetic nanoparticles (CS MNPs) at various sizes were synthesized for targeted delivery of Doxorubicin (Fig. 1). Cellular internalization and cytotoxic effect of Doxorubicin-loaded CS MNPs were investigated on MCF-7 and Doxorubicin resistant MCF-7 (MCF-7/Dox) cell lines. Chemical and physical characterizations of synthesized nanoparticles and their cytotoxicity on MCF-7/Dox cell line have indicated that they can be suitable for pH sensitive targeted delivery system for Doxorubicin.

2. Materials and methods

2.1. Materials

Iron(II) chloride tetrahydrate ($\text{FeCl}_2 \cdot 4\text{H}_2\text{O}$), iron(III) chloride hexahydrate ($\text{FeCl}_3 \cdot 6\text{H}_2\text{O}$) and ammonium hydroxide (NH_4OH) were obtained from Merck, Germany. Chitosan (low molecular weight) was purchased from Sigma–Aldrich, Saint Louis, USA and sodium tripolyphosphate (TPP) was from Sigma–Aldrich Chemie GmbH, Germany.

The parental MCF-7 human breast cancer cell line was donated by the ŞAP Institute, Ankara, Turkey. 1 μM Doxorubicin Resistant

MCF-7 cell line (MCF-7/Dox) was previously developed from MCF-7 cells (MCF-7/S) by continuous drug applications in our laboratory (Kars et al., 2006). RPMI medium and fetal bovine serum (FBS) were obtained from Biochrom AG, Germany. Trypsin–EDTA, trypan blue and XTT Cell Proliferation Kit were purchased from Biological Industries, Israel. Phosphate buffered saline (PBS) and dimethyl sulfoxide (DMSO) were obtained from Sigma–Aldrich, USA.

2.2. In situ synthesis of chitosan coated magnetic iron oxide nanoparticles

Chitosan coated magnetic iron oxide nanoparticles (CS MNPs) (Fig. 1b) were synthesized by co-precipitation of Fe(II) and Fe(III) salts at a 1:2 ratio in 150 ml deionized water within a five necked glass flask in the presence of chitosan and tripolyphosphate (TPP) molecules (Kavaz et al., 2010). Unsoy et al. (2012) reported that during the nucleation of Fe_3O_4 , chitosan molecules wrap these anionic cores and TPP cross-links the chitosan molecules around Fe_3O_4 cores in the in situ synthesis method. This method was optimized by changing the NH_4OH concentrations in order to obtain different sized CS MNPs. The diameters of CS MNPs were found as 103 nm for S_1 , 86 nm for S_2 , 66 nm for S_3 and 58 nm for S_4 according to DLS analyses. The sizes of the nanoparticles decrease proportional to the increase of NH_4OH concentration during the synthesis.

2.3. Characterization of chitosan coated magnetic iron oxide nanoparticles

X-ray diffraction (XRD), X-ray photoelectron spectroscopy (XPS/ESCA), Vibrating Sample Magnetometer (VSM), Fourier transform infrared spectroscopy (FTIR), transmission electron microscopy (TEM), dynamic light scattering (DLS), and thermal gravimetric analysis (TGA) analyses were employed to investigate the properties of different sized chitosan coated iron oxide nanoparticles previously (Unsoy et al., 2012).

2.4. Loading of Doxorubicin on chitosan coated magnetic iron oxide nanoparticles

Doxorubicin loading was carried on the synthesized CS MNPs (S_1 – S_4) with various drug concentrations in potassium phosphate buffer ($\text{K}_2\text{HPO}_4/\text{KH}_2\text{PO}_4$), in order to obtain the highest loading efficiency. The mixture of CS MNPs (2.5 mg/ml), Doxorubicin and

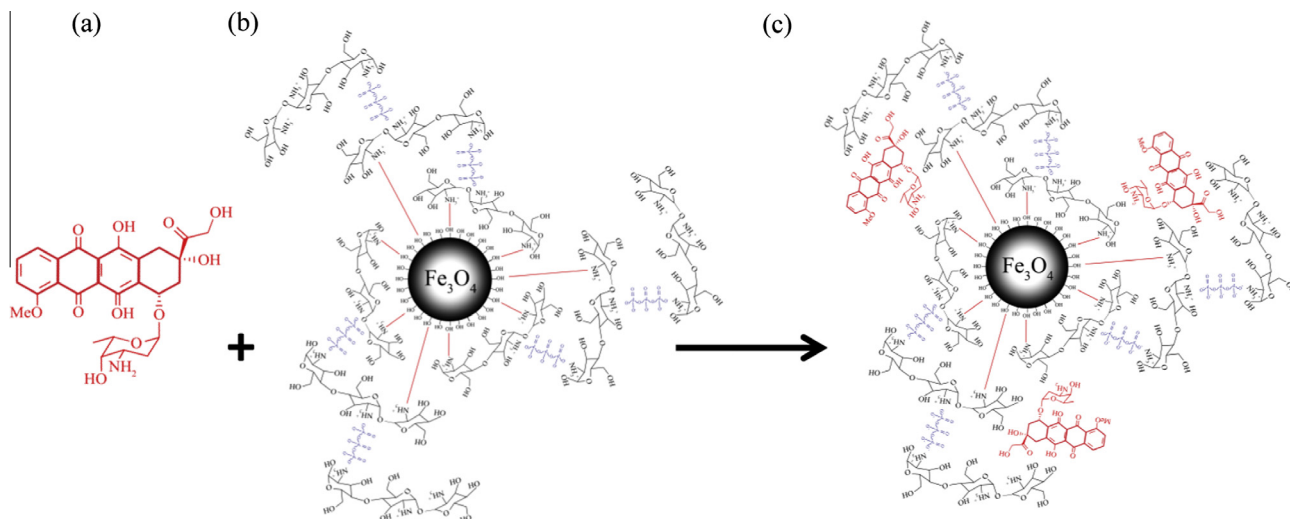


Fig. 1. Molecular formulas of Doxorubicin (a), CS MNP (b) and schematic representation of Doxorubicin loaded CS MNP (c).

potassium phosphate buffer was rotated (Biosan Multi RS-60 Rota-tor) at 90 rpm with 5 s vibration intervals for 24 h in the light protected tubes at room temperature. Then, Doxorubicin loaded CS MNPs were separated by magnetic decantation. The loading efficiency was quantified by measuring the absorbance values of unloaded drug in the supernatant with a UV-spectrophotometer at 481 nm (Eq. (1)). The Doxorubicin loading was also confirmed by FTIR analyses. The schematic representation of Doxorubicin loaded CS MNPs were given in Fig. 1c.

$$\text{Loading Efficiency(\%)} = \frac{(\text{total } \mu\text{g of drug added}) - (\mu\text{g of drug in supernatant})}{(\text{total } \mu\text{g of drug added})} \times 100 \quad (1)$$

2.5. Release of drug from Doxorubicin loaded CS MNPs

Doxorubicin release profiles of 400 and 500 $\mu\text{g/ml}$ drug loaded CS MNPs were determined in buffers at pH 4.2 and pH 5.0, up to 30 h at 37 °C. The release of drug from CS MNPs was determined by measuring the absorbance of the released Doxorubicin in the supernatant within time intervals at 481 nm by a UV-spectrophotometer. Supernatant was obtained with magnetic decantation of CS MNPs. Quantification of Doxorubicin was performed by generating a calibration curve with known amounts of drug concentrations.

2.6. Stability of Doxorubicin loaded CS MNPs

The stability of CS MNPs loaded with highest amounts of Doxorubicin was determined in potassium phosphate buffer (pH 7.4) up to eight weeks at 37 °C. The amount of released Doxorubicin from the nanoparticles was measured by the absorbance at 481 nm.

2.7. Cellular internalization of Doxorubicin loaded CS MNPs

Doxorubicin (500 $\mu\text{g/ml}$) loaded CS MNPs were applied on MCF-7 and MCF-7/Dox cell lines for 24 h. The cells treated with Doxorubicin loaded CS MNPs were washed three times with PBS and the cellular internalization of nanoparticles was observed by fluorescence microscopy. Images were also acquired after the addition of DAPI for cell nuclei staining.

2.8. Cytotoxicity analysis of Doxorubicin loaded CS MNPs

Cytotoxicity of Doxorubicin and Doxorubicin loaded CS MNPs were determined by XTT cell proliferation assay. MCF-7 and MCF-7/Dox cells were treated with free Doxorubicin (Dönmez, 2010) and Doxorubicin loaded CS MNPs (highest drug doses are 5 μM and 75 μM Doxorubicin containing nanoparticles for MCF-7 and MCF-7/Dox cells, respectively) in 96-well plates. After 48 h of incubation, cell viability profiles and IC_{50} (half maximal inhibitory concentration) values were determined for each particular cell type.

3. Results

3.1. Characterization of chitosan coated magnetic iron oxide nanoparticles

Characterizations of different sized CS MNPs were performed by XRD, XPS/ESCA, FTIR, TEM, DLS, and TGA analyses (Unsoy et al., 2012). It was observed that the mass ratio of chitosan in the synthesized nanoparticles was found about 23% (S_1), 20% (S_2), 17% (S_3), and 15% (S_4) by TGA analyses. The synthesized CS MNPs have a spherical and uniform size distribution in TEM images as

reported previously (Unsoy et al., 2012). The average diameters are around 6–8 nm (S_1), 5–7 nm (S_2), 3–5 nm (S_3), and 1–3 nm (S_4) (Fig. 2a and b). TEM images usually indicate only the core sizes of CS MNPs because of the collapse of chitosan polymer on the MNPs surface during the evaporation of the dispersion medium prior to imaging. On the other hand, DLS analyses measure the hydrodynamic size of nanoparticles in the dispersion medium and the average sizes were found much larger due to the swelling of the polymer around the magnetic core (Fig. 2c and d).

3.2. Doxorubicin loading on CS MNPs

Doxorubicin loading studies were initially performed on CS MNP- S_1 with different drug concentrations in phosphate buffer (pH 6). In order to determine the highest loading efficiency, Doxorubicin concentration gradually increased up to 600 $\mu\text{g/ml}$ where the saturation was obtained. The loading efficiencies of 150 $\mu\text{g/ml}$, 300 $\mu\text{g/ml}$, 400 $\mu\text{g/ml}$, 500 $\mu\text{g/ml}$ and 600 $\mu\text{g/ml}$ Doxorubicin were 99%, 98%, 98%, 96% and 81%, respectively. The most efficient and highest amount of loaded Doxorubicin was achieved with 96% loading efficiency as 481 $\mu\text{g/ml}$ (Table 1).

The FTIR analyses were performed in order to support the Doxorubicin loading efficiency on CS MNPs. The FTIR spectrum of Doxorubicin shows multiple peaks at 2932 (C–H), 1730 (C O), 1618 and 1577 (N–H), 1414 (C–C) and 1071 (C–O) cm^{-1} . These peaks are also present in the FTIR spectrum of Doxorubicin loaded CS MNPs as shifted to 2920 (C–H), 1717 (C O), 1614 and 1574 (N–H), 1406 (C–C) and 1030 (C–O) cm^{-1} , respectively (Fig. 3). These results indicate that Doxorubicin was successfully loaded onto the CS MNPs.

Doxorubicin loading efficiencies of 400 $\mu\text{g/ml}$ and 500 $\mu\text{g/ml}$ Doxorubicin on CS MNPs (S_{1-4}) were determined. The loading efficiencies on nanoparticles at 400 $\mu\text{g/ml}$ Doxorubicin were about 98% for S_1 , 92% for S_2 , 90% for S_3 and 88% for S_4 , and at 500 $\mu\text{g/ml}$; 97% for S_1 , 91% for S_2 , 90% for S_3 and 88% for S_4 Fig. 4. The highest Doxorubicin loading efficiency was obtained in S_1 , which contains the highest amount of chitosan (23%) and has the largest particle size (103 nm). This may be due to the fact that Doxorubicin was loaded into the chitosan layer.

3.3. Doxorubicin release from the nanoparticles

Doxorubicin release profiles and stability analyses of chitosan coated magnetic nanoparticles were studied by considering different parameters such as pH, buffer type, temperature and size of nanoparticles. S_1 and S_4 were selected for drug release and stability studies because of their size differences. Doxorubicin release was investigated at different pH values (pH 4.2 and 5.0) which mimic endosomal conditions.

In 500 $\mu\text{g/ml}$ and 400 $\mu\text{g/ml}$ initial Doxorubicin loading concentrations, S_1 nanoparticles released about 61% and 53% of the loaded drug respectively during the first 15 h at pH 4.2 (Fig. 5). On the other hand, 75% (500 $\mu\text{g/ml}$) and 64% (400 $\mu\text{g/ml}$) of Doxorubicin was released from S_4 , under the same conditions (Fig. 6).

In pH 5.0, drug release rate of S_1 was 35% and 30% at 500 $\mu\text{g/ml}$ and 400 $\mu\text{g/ml}$ loading concentrations of Doxorubicin for 15 h, respectively (Fig. 5). The drug release rate in case of S_4 was 47% and 40% at 500 $\mu\text{g/ml}$ and 400 $\mu\text{g/ml}$ concentrations of Doxorubicin (Fig. 5). A burst release of Doxorubicin from CS MNPs was observed at the initial stage of 30 min at pH 4.2 as 20–30% and at pH 5.0 as 15–20%. Then a slower release was observed after 7 h (Figs. 5 and 6).

The pH value of the medium has a remarkable effect on the release of Doxorubicin from the chitosan coated nanoparticles. Drug release rates of CS MNPs were significantly different. The

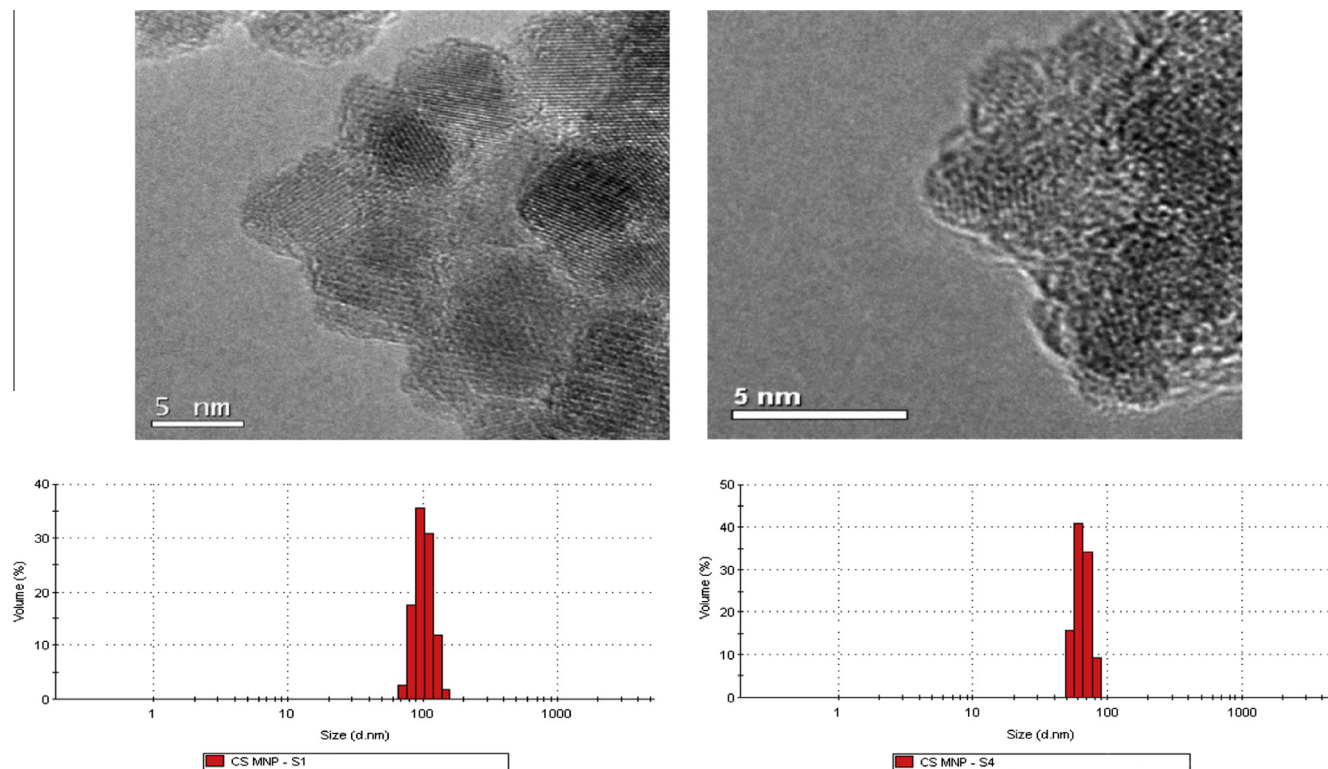


Fig. 2. TEM images (a and b) and DLS size graphs (c and d) of CS MNP-S₁ and -S₄, respectively.

Table 1

Loading efficiencies on CS MNP-S₁ at different concentrations (150–600 µg/ml) of Doxorubicin. Each data represents the mean ± S.D. (n = 3).

Loading efficiencies and loaded amounts of Doxorubicin on CS MNP-S ₁					
Doxorubicin concentration (µg/ml)	150	300	400	500	600
Loaded amount of Doxorubicin (µg/ml)	149 ± 0.2	295 ± 0.7	392 ± 1.4	481 ± 2.9	486 ± 1.8
Doxorubicin loading efficiency	99%	98%	98%	96%	81%

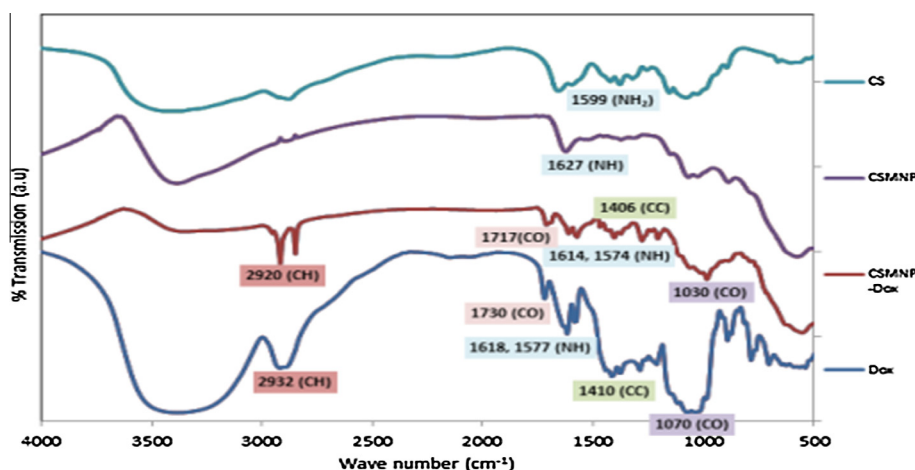


Fig. 3. FTIR spectra of CS (a), CS MNPs (b), Doxorubicin loaded CS MNPs (c), and Doxorubicin (d).

release of Doxorubicin was quite higher at pH 4.2 than pH 5 for both S₁ and S₄ CS MNPs (Figs. 5 and 6).

In terms of drug release characteristics, there is only about 10% difference was observed between S₁ and S₄ nanoparticles. These results are in parallel with the drug loading amounts of nanoparticles.

3.4. Stability of Doxorubicin-loaded nanoparticles

The stability of Doxorubicin loaded nanoparticles was evaluated up to 8 weeks in phosphate buffer (pH 7.4) at 37 °C, which mimics the physiological conditions (Fig. 7). Results show that the stability of 400 µg/ml and 500 µg/ml Doxorubicin loaded S₁ and S₄

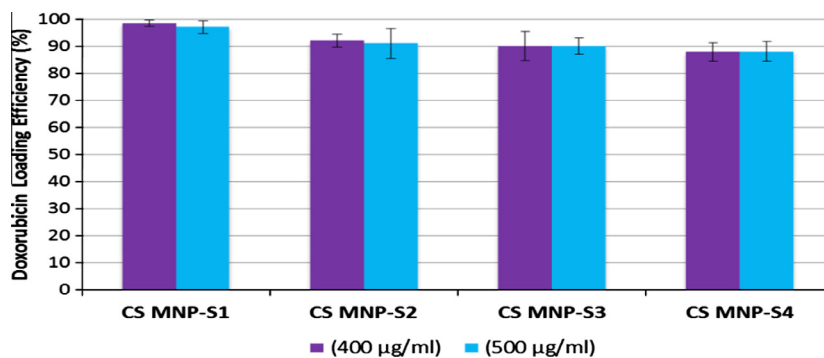


Fig. 4. Doxorubicin loading efficiency on S_1 , S_2 , S_3 and S_4 at the highest loaded amounts of Doxorubicin concentrations. Each data represents the mean \pm S.D. ($n = 3$).

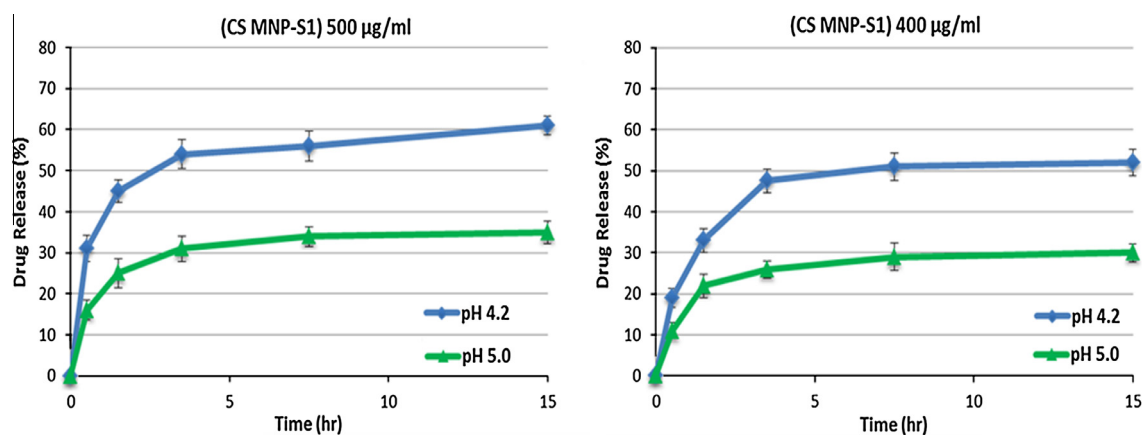


Fig. 5. Doxorubicin release graph of S_1 nanoparticles at pH 4.2 and 5.0 with 500 µg/ml and 400 µg/ml initial loading concentrations. Each data represents the mean \pm S.D. ($n = 3$).

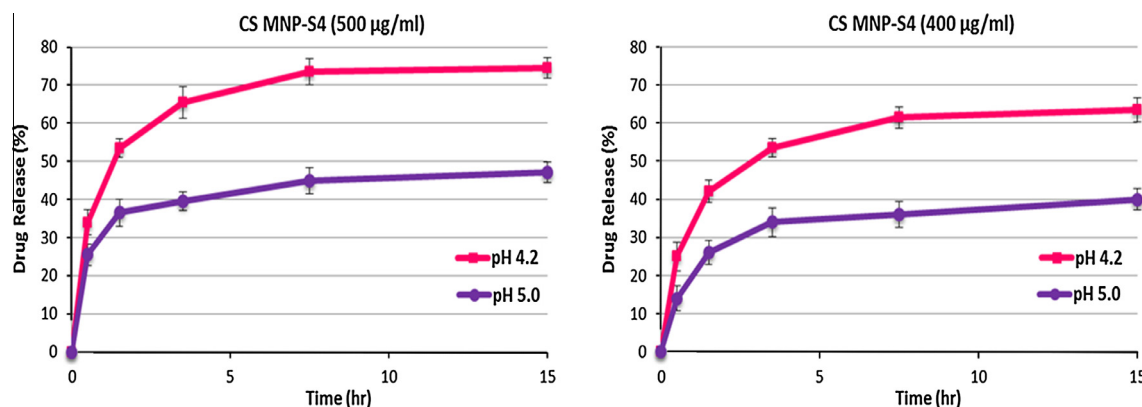


Fig. 6. Doxorubicin release of S_4 nanoparticles at pH 4.2 and 5.0 with 500 µg/ml and 400 µg/ml initial Doxorubicin loading concentrations. Each data represents the mean \pm S.D. ($n = 3$).

nanoparticles was around 80–85% stable for both 37 °C and 4 °C at pH 7.4. The stability of nanoparticles did not significantly change with temperature. Results indicated that Doxorubicin loaded CS MNPs were quite stable at both 37 °C and 4 °C (pH 7.4), which can be stored safely.

3.5. Cellular internalization of Doxorubicin-loaded nanoparticles

Internalization of Doxorubicin loaded CS MNP- S_1 nanoparticles were investigated by fluorescence microscopy on MCF-7 and MCF-7/Dox cells. The obtained images are given in Fig. 8. Doxorubicin is

a fluorescent chemical, having a bright red color when visualised with red filter. In Fig. 8a, c, d, and f, red color indicates that Doxorubicin loaded nanoparticles were internalized the cells, reflecting the concentrations of nanoparticles in the cells. The nuclei of the cells are specifically visualized with DAPI staining (Fig. 8b and e). Free Doxorubicin does not sufficiently accumulate in Doxorubicin resistant MCF-7 cells (Fig. 8f). On the other hand Doxorubicin loaded nanoparticles accumulate in the cytoplasm of the resistant cells at high amounts similar to the sensitive cells (Fig. 8d). The cellular uptake of nanoparticles could be facilitated by the positive surface charges of chitosan coat.

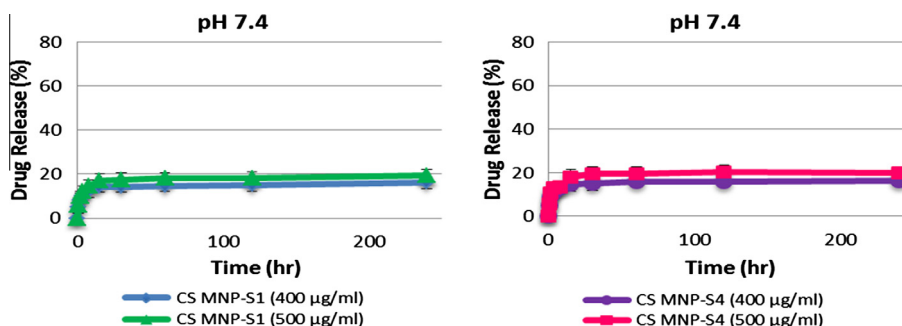


Fig. 7. Stability of Doxorubicin (400–500 µg/ml) loaded CS MNP-S₁ and CS MNP-S₄ in phosphate buffer (pH = 7.4) up to 8 weeks. Each data represents the mean ± S.D. (n = 3).

3.6. Cytotoxicity analysis of Doxorubicin loaded CS MNPs

The cytotoxic effect of CS MNPs without Doxorubicin have previously investigated and the results showed that the nanoparticles are not toxic (Unsoy et al., 2012). Fig. 9 demonstrates the anti-proliferative effects of Doxorubicin loaded CS MNPs at increasing concentrations on MCF-7 and MCF-7/Dox cells. IC₅₀ values of Doxorubicin loaded nanoparticles were identified as 1.0 µM and 13.5 µM on MCF-7 and MCF-7/Dox cells, respectively. However, IC₅₀ values were obtained as 1.6 µM and 176 µM for free Doxorubicin in the MCF-7 and resistant MCF-7 cells, respectively. Previously the IC₅₀ values of free Doxorubicin were found as 1.8 µM and 202.5 µM in the sensitive and resistant MCF-7 cells (Dönmez, 2010). The graph showing IC₅₀ values of free Doxorubicin and Doxorubicin loaded CS MNPs on MCF-7 and MCF-7/Dox cells were given in Fig. 9. The cell proliferation decreases with increasing concentrations of Doxorubicin loaded CS MNPs. Thus, the efficacy of Doxorubicin increases when loaded on CS MNPs. The decrease in IC₅₀ value is more significant in case of Doxorubicin resistant cells. As it is seen from Fig. 9, the IC₅₀ value decreased about 13 folds in case of Doxorubicin loaded CS MNPs, compared to free Doxorubicin.

It is known that Doxorubicin is extruded out of the cell by P-glycoprotein (multidrug resistance protein-1), which acts as a pump in drug resistant cells (Riganti et al., 2011). It would be possible to overcome MDR-1-related resistance by releasing the drug in low pH away from the cell membrane and efflux pumps

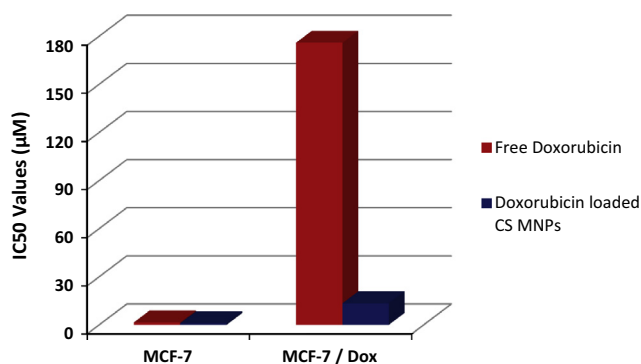


Fig. 9. The graph of IC₅₀ values display the comparison between the efficacy of free Doxorubicin and Doxorubicin loaded CS MNPs on MCF-7 and MCF-7/Dox cells.

(Khodadust et al., 2013). It was demonstrated that Doxorubicin loaded CS MNPs were 13-fold more toxic on Doxorubicin resistant MCF-7 cells compared with free Doxorubicin. These results confirmed that the loaded and released Doxorubicin were active and cause to overcome the drug resistance.

4. Discussion

The synthesis of chemotherapeutic loaded CS MNPs for magnetic field targeted drug delivery is a fairly novel subject of

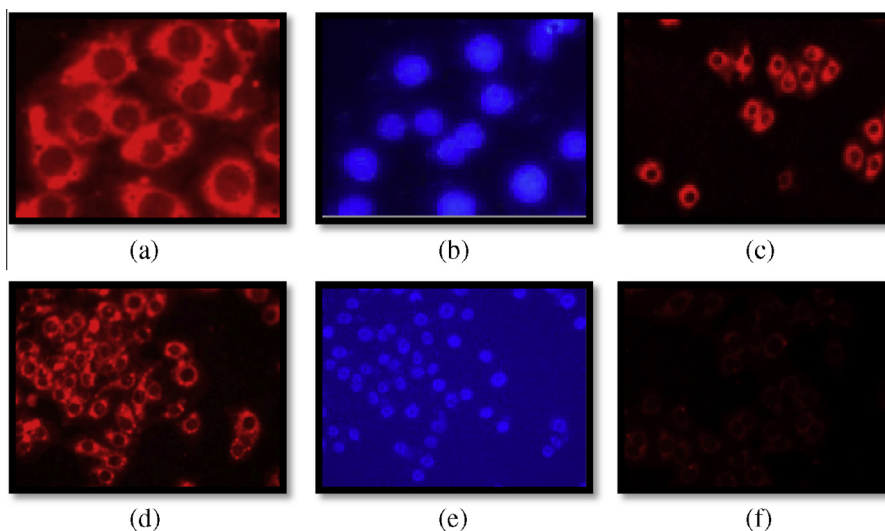


Fig. 8. The fluorescent microscopy images. (a) Doxorubicin loaded CS MNPs were internalized by MCF-7 cells, (b) DAPI stain labelled nuclei of the cells, (c) fluorescence of internalized free Doxorubicin inside the MCF-7 cells, (d) fluorescence of internalized Doxorubicin loaded CS MNPs inside the MCF-7/Dox resistant cells, (e) DAPI stain labelled nuclei of the MCF-7/Dox resistant cells, (f) free Doxorubicin cannot accumulate inside the MCF-7/Dox resistant cells as much as MCF-7 cells.

research. However, Yuan et al. (2010) have synthesized Doxorubicin loaded chitosan grafted copolymer coated magnetic nanoparticles for targeted drug delivery; they did not perform a detailed investigation on nanoparticle characterization and their cellular uptake.

The size-tunable synthesis of CS MNPs was performed by in situ coprecipitation method (Unsoy et al., 2012). This method is very advantageous for biomedical applications than the other methods because of the simple and mild synthesis conditions (Tiyaboanchai and Limpeanchob, 2007). The nanoparticles obtained by in situ coprecipitation method have higher biocompatibility and biodegradability than covalently cross-linked chitosan (Agnihotri et al., 2004; Park et al., 2010). The average diameters of synthesized CS MNPs (S₁–S₄) differ according to TEM and DLS measurements. Bhattarai et al. (2008) reported that the difference between the diameters obtained by DLS and TEM, reflects the size of chitosan layer for nanoparticles smaller than ≤ 200 nm (Bhattarai et al., 2008; Unsoy et al., 2012).

The FTIR results supported that the Doxorubicin loading on CS MNPs was successfully achieved (Kayal and Ramanujan, 2010; Yuan et al., 2010). The highest loading efficiency was obtained for CS MNP-S₁ nanoparticles (97–98%). This may be due to the highest chitosan content of CS MNP-S₁ (Unsoy et al., 2012).

Drug release mechanisms of nanoparticles has been well described in the literature as (i) desorption, (ii) diffusion, and (iii) matrix degradation (Aydın and Pulat, 2012). Chitosan is known to exhibit pH-dependent swelling and controlled drug release properties (Berger et al., 2004). In this study, the swelling of unloaded CS MNPs was more than the loaded ones. The drug diffuses into the nanoparticles and forms more cross-linking sites in the chitosan structure which leads to lower swelling of the nanoparticles as explained by Shu and Zhu (2002). As in the study of Sahu et al. (2010) the pH value of dissolution medium affected the release rates of Doxorubicin. The drug release rate of CS MNPs increased with the reduced pH value of dissolution medium. This release behaviour would be attributed to the higher solubility of Doxorubicin and degradation of chitosan at acidic pHs.

For the successful delivery of Doxorubicin, the stability of CS MNPs at physiological conditions and efficient drug release at the targeted tumor site is required (Gillies and Fréchet, 2005). The drug release is achieved with the swelling behaviour of chitosan due to its pH sensitivity. Charge density on the surface of the nanoparticles is important in electrostatic interactions and mainly depends on the solution pH. Swelling of the chitosan and release of the drug is mainly influenced by ionic interactions between chitosan chains; which depend on the cross-linking density of the chitosan network (Berger et al., 2004). As a result, pH responsive drug carriers provide selective drug release at acidic intracellular vesicles such as endosomes and lysosomes in targeted tumor cells (Estrella et al., 2013).

Synthesized CS MNPs are stable at physiological conditions (pH 7.4). These Nanoparticles are expected to have an effective drug release in the tumor microenvironment since the drug release rate accelerates with the decrease in pH (around 4.0–5.0). The pH of the tumor microenvironment is low (around 4.0–5.5) due to the high anaerobic glucose metabolism of cancer cells (Decuzzi and Ferrari, 2007; Engin et al., 1995; Ojugo et al., 1999; Van et al., 1999). It is considered that the nanoparticles are taken up by endocytosis into the cells (Mellman et al., 1986; Park et al., 2006) and this endocytic pathway begins near the physiological pH of 7.4, then it drops to pH 5.5–6.0 in endosomes and comes around pH 4.5 in lysosomes (Sahu et al., 2010). Therefore, it is expected that, CS MNPs will be responsive to pH and selectively release its drug load in the tumor cells of the targeted tissue. According to the drug release profiles of CS MNPs, the loaded Doxorubicin is mostly released within the first 7 h. At the end of 7 h Doxorubicin release

was higher at pH 4.2 (70%) than at pH 5 (45%). CS MNPs showed an initial burst release of Doxorubicin in the range of 10–20% and 15–35% for 400 $\mu\text{g/ml}$ and 500 $\mu\text{g/ml}$ loading concentrations, respectively at acidic pH values (pH 4.2 and 5) during a period of 30 min. This initial rapid release, characterized as “burst effect”, occurs by desorption of Doxorubicin, localized on the surface of nanoparticles. After this initial burst effect, a slower and controlled release occurred throughout the incubation period. The drug release rate was approximately 10% higher in S₄ CS MNPs with respect to S₁ due to the lower chitosan content. S₁ has more chitosan content and therefore, it has higher drug loading and retention capacity. The Doxorubicin loading profiles of S₁ and S₄ CS MNPs were quite similar. The S₄ has larger surface area than S₁. However its chitosan content is less than S₁.

Doxorubicin loaded CS MNPs are successfully internalized by both sensitive and Doxorubicin resistant MCF7 cells. Normally Doxorubicin does not effectively accumulate in the cytoplasm of the drug resistant MCF-7 cells due to the high expression of P-glycoprotein (P-gp) on the cell membrane (Dönmez, 2010). Internalization mechanisms of free Doxorubicin and CS MNPs are different. While free Doxorubicin diffuses through the cell membrane, CS MNPs are taken up by endocytosis into the cells. Thus, when Doxorubicin is loaded into the nanoparticles, P-gp cannot pump out of the drug and Doxorubicin can accumulate in the cells.

According to the previous studies carried out in our laboratory, resistant MCF-7/Dox cells are approximately 110 fold more resistant to Doxorubicin than sensitive MCF-7 cells (Dönmez, 2010). In order to overcome the resistance by improving drug influx via escaping from P-gp pump; Doxorubicin was loaded on CS MNPs. The XTT results of our study show that IC₅₀ values of free Doxorubicin (176 μM) decreased to 13.5 μM when Doxorubicin was loaded into the CS MNPs. Consequently, loading of Doxorubicin onto the nanoparticles not only 13-fold increased the efficiency of drug but also overcame the resistance to Doxorubicin in MCF-7/Dox cells.

On the other hand, the difference between the IC₅₀ values of free Doxorubicin and Doxorubicin loaded on CS MNPs is not drastic in MCF-7 cells in comparison to resistant subline. This is due to both free Doxorubicin and Doxorubicin loaded CS MNPs were efficiently internalized by the MCF-7 cells.

These nanoparticles can be given through either intratumoral or intravenous administration and targeted to the tumor tissue under magnetic field. The defining characteristics of long circulating nanoparticles in the blood stream are charge, size (10–100 nm), hydrophobicity and immunogenicity of particles (Bisht and Amarnath, 2009). CS MNPs have neutral charge due to the ionic interactions between the drug and nanoparticles. The hydrodynamic size of CS MNPs is in this range. Since CS MNPs are biocompatible and have hydrophilic surfaces, they circulate at a prolonged time in the blood stream.

5. Conclusion

In summary, in this study, different sized CS MNPs were synthesized and efficiently loaded with Doxorubicin for the *in vitro* targeted delivery applications on MCF-7 breast cancer cells. The optimal loading efficiency, stability and release profiles of Doxorubicin loaded nanoparticles were determined. The Doxorubicin release profiles showed a pH dependent, and slow release pattern. As the pH decreased, swelling ratio of chitosan increased, therefore the drug release increased. The CS MNPs released most of the Doxorubicin at pH 4.2, while the nanoparticles are quite stable at pH 7.4.

Fluorescence microscopy images have revealed that Doxorubicin loaded CS MNPs were taken up by the cells and accumulated

around the nucleus, so that Doxorubicin is successfully delivered near to the nucleus, where the drug shows its anti-cancer activity. Doxorubicin loaded CS MNPs were more toxic on Doxorubicin resistant MCF-7 cells than free drug. This confirms that the released drug is active. Application of Doxorubicin as loaded on CS MNPs caused the reversal of drug resistance by increasing the accumulation of Doxorubicin in the cells. According to these results, it is inferred that the synthesized chitosan coated magnetic nanoparticles has a high potential to be used as a pH responsive drug delivery system, which can be targeted to tumor cells under magnetic field and seems to be an efficient system to eliminate Doxorubicin resistance in MCF-7/Dox cells.

References

- Agnihotri, S.A., Mallikarjuna, N.N., Aminabhavi, T.M., 2004. Recent advances on chitosan-based micro- and nanoparticles in drug delivery. *J. Control. Release* 100, 5–28.
- Andrade, F., Antunes, F., da Silva, A.N.S., das Neves, J., Ferreira, D., Sarmiento, B., 2011. Chitosan formulations as carriers for therapeutic proteins. *Curr. Drug Discov. Technol.* 8, 157–172.
- Aydin, R.S.T., Pulat, M., 2012. 5-Fluorouracil encapsulated chitosan nanoparticles for pH-stimulated drug delivery: evaluation of controlled release kinetics. *J. Nanomater.* 313961, 1–10.
- Berger, J., Reist, M., Mayer, J.M., Felt, O., Peppas, N.A., Gurny, R., 2004. Structure and interactions in covalently and ionically crosslinked chitosan hydrogels for biomedical applications. *Eur. J. Pharm. Biopharm.* 57 (1), 19–34.
- Bhattacharai, S.R., Kc, R.B., Kim, S.Y., Sharma, M., Khil, M.S., Hwang, P.H., Chung, G.H., Kim, H.Y., 2008. N-hexanoyl chitosan stabilized magnetic nanoparticles: implication for cellular labeling and magnetic resonance imaging. *J. Nanobiotechnol.* 6, 1.
- Bisht, S., Amarnath, M., 2009. Dextran–doxorubicin/chitosan nanoparticles for solid tumor therapy. *Wiley Interdisciplin. Rev.: Nanomed. Nanobiotechnol.* 1 (4), 415–425.
- Dash, M., Chiellini, F., Ottenbrite, R.M., Chiellini, E., 2011. Chitosan: a versatile semi-synthetic polymer in biomedical applications. *Prog. Polym. Sci.* 36, 981–1014.
- Decuzzi, P., Ferrari, M., 2007. The role of specific and non-specific interactions in receptor-mediated endocytosis of nanoparticles. *Biomaterials* 28, 2915–2922.
- Dodane, V., Vilivalam, V.D., 1998. Pharmaceutical applications of chitosan. *Pharm. Sci. Technol. Today* 1, 246–253.
- Dönmez, Y., 2010. Reversal of multidrug resistance by small interfering RNAs (siRNA) in Doxorubicin resistant MCF-7 breast cancer cells. M.Sc. Thesis METU, Ankara, Turkey.
- Engin, K., Leeper, D.B., Cater, J.R., Thistlethwaite, A.J., Tupchong, L., McFarlane, J.D., 1995. Extracellular pH distribution in human tumors. *Int. J. Hyperth.* 11, 211–216.
- Estrella, V., Chen, T., Lloyd, M., Wojtkowiak, J., Cornnell, H.H., Hashim, A.I., Bailey, K., Balagurunatham, Y., Rothberg, J.M., Sloane, B.F., Johnson, J., Gatenby, R.A., Gillies, R.J., 2013. Acidity generated by the tumor microenvironment drives local invasion. *Cancer Res.* 73, 1524–1535.
- Gillies, E.R., Fréchet, J.M., 2005. PH-responsive copolymer assemblies for controlled release of Doxorubicin. *Bioconjug. Chem.* 16, 361–368.
- Grenha, A., 2012. Chitosan nanoparticles: a survey of preparation methods. *J. Drug Target.* 20, 291–300.
- Gupta, A.K., Naregalkar, R.R., Vaidya, V.D., Gupta, M., 2007. Recent advances on surface engineering of magnetic iron oxide nanoparticles and their biomedical applications. *Nanomedicine* 2, 23–39.
- Kars, M.D., Iseri, O.D., Gunduz, U., Ural, A.U., Arpacı, F., Molnar, J., 2006. Development of rational in vitro models for drug resistance in breast cancer and modulation of MDR by selected compounds. *Anticancer Res.* 26, 4559–4568.
- Kavaz, D., Odabas, S., Demirbilek, M., Güven, E.Ö., Denkbaş, E.B., 2010. Bleomycin loaded magnetic chitosan nanoparticles as multifunctional nanocarriers. *J. Bioactive Compatib. Polym.* 25, 305–318.
- Kayal, S., Ramanujan, R.V., 2010. Doxorubicin loaded PVA coated iron oxide nanoparticles for targeted drug delivery. *Mater. Sci. Eng., C* 30, 484–490.
- Khodadust, R., Mutlu, P., Yalcin, S., Unsoy, G., Gunduz, U., 2013. Doxorubicin loading, release, and stability of polyamidoamine dendrimer-coated magnetic nanoparticles. *J. Pharm. Sci.* 102.6, 1825–1835.
- Lim, E.K., Huh, Y.M., Yang, J., Lee, K., Suh, J.S., Haam, S., 2011. PH-triggered drug-releasing magnetic nanoparticles for cancer therapy guided by molecular imaging by MRI. *Adv. Mater.* 23, 2436–2442.
- Liu, Z., Jiao, Y., Wang, Y., Zhou, C., Zhang, Z., 2008. Polysaccharides-based nanoparticles as drug delivery systems. *Adv. Drug Deliv. Rev.* 60, 1650–1662.
- Longhi, A., Ferrari, S., Bacci, G., Specchia, S., 2007. Long-term follow-up of patients with doxorubicin-induced cardiac toxicity after chemotherapy for osteosarcoma. *Anticancer Drugs* 18, 737–744.
- Maeda, H., 2001. The enhanced permeability and retention (EPR) effect in tumor vasculature: the key role of tumor-selective macromolecular drug targeting. *Adv. Enzyme Regul.* 41, 189–207.
- Mellman, I., Fuchs, R., Helenius, A., 1986. Acidification of the endocytic and exocytic pathways. *Annu. Rev. Biochem.* 55, 773–800.
- Ojugo, A.S.E., Mesheehy, P.M.J., McIntyre, D.J.O., McCoy, C., Stubbs, M., Leach, M.O., Judson, I.R., Griffiths, J.R., 1999. Measurement of the extracellular pH of solid tumors in mice by magnetic resonance spectroscopy: a comparison of exogenous 19F and 31P probes. *NMR Biomed.* 12, 495–504.
- Park, J.S., Han, T.H., Lee, K.Y., Han, S.S., Hwang, J.J., Moon, D.H., Kim, S.Y., Cho, Y.W., 2006. N-acetyl histidine-conjugated glycol chitosan self-assembled nanoparticles for intracytoplasmic delivery of drugs: endocytosis, exocytosis and drug release. *J. Control. Release* 115, 37–45.
- Park, Y., Kang, E., Kwon, O.J., Park, H.K., Kim, J.H., Yun, C.O., 2010. Tumor targeted adenovirus nanocomplex ionically crosslinked by chitosan. *J. Control. Release* 148, e124.
- Riganti, C., Voena, C., Kopecka, J., Corsetto, P.A., Montorfano, G., Enrico, E., Costamagna, C., Rizzo, A.M., Ghigo, D., Bosia, A., 2011. Liposome-encapsulated doxorubicin reverses drug resistance by inhibiting P-glycoprotein in human cancer cells. *Mol. Pharm.* 8 (3), 683–700.
- Rodrigues, S., Dionisio, M., López, C.R., Grenha, A., 2012. Biocompatibility of chitosan carriers with application in drug delivery. *J. Funct. Biomater.* 3, 615–641.
- Sahu, S.K., Mallick, S.K., Santra, S., Maiti, T.K., Ghosh, S.K., Pramatik, P., 2010. In vitro evaluation of folic acid modified carboxymethyl chitosan nanoparticles loaded with doxorubicin for targeted delivery. *J. Mater. Sci. – Mater. Med.* 21, 1587–1597.
- Shu, X.Z., Zhu, K.J., 2002. The influence of multivalent phosphate structure on the properties of ionically cross-linked chitosan films for controlled drug release. *Eur. J. Pharm. Biopharm.* 54, 235–243.
- Strebhardt, K., Ullrich, A., 2008. Paul Ehrlich's magic bullet concept: 100 years of progress. *Nat. Rev. Cancer* 8, 473–480.
- Sun, C., Lee, J.S.H., Zhang, M.Q., 2008. Magnetic nanoparticles in MR imaging and drug delivery. *Adv. Drug Deliv. Rev.* 60, 1252–1265.
- Tan, M.L., Choong, P.F.M., Dass, C.R., 2009. Review: doxorubicin delivery systems based on chitosan for cancer therapy. *J. Pharm. Pharmacol.* 61, 131–142.
- Tiyaboanchai, W., Limpeanchob, N., 2007. Formulation and characterization of amphotericin B-chitosan-dextran sulfate nanoparticles. *Int. J. Pharm.* 329, 142–149.
- Unsoy, G., Yalcin, S., Khodadust, R., Gunduz, G., Gunduz, U., 2012. Synthesis optimization and characterization of chitosan-coated iron oxide nanoparticles produced for biomedical applications. *J. Nanopart. Res.* 14, 964–968.
- Van, R.S., Bhujwalla, Z.M., Ballerteros, P., Alvarez, J., Cerdan, S., Galons, J.P., Gillies, R.J., 1999. In vivo imaging of extracellular pH using 1H MSRI. *Magn. Reson. Med.* 41, 743–750.
- Wood, J., 2002. Doxorubicin. In: Allwood, M. et al. (Eds.), *The Cytotoxics Handbook*, fourth ed. Radcliffe Medical Press, Oxford, pp. 322–329.
- Yuan, Q., Shah, J., Hein, S., Misra, R.D., 2010. Controlled and extended drug release behavior of chitosan-based nanoparticle carrier. *Acta Biomater.* 6, 1140–1148.
- Zeng, X., Ralf, M., Andreas, M.N., 2014. Nanoparticle-directed sub-cellular localization of doxorubicin and the sensitization breast cancer cells by circumventing GST-mediated drug resistance. *Biomaterials* 35 (4), 1227–1239.